Preliminary Identification of Flow Regimes in a Mechanically Oscillated Planar Jet

M. Riese, G.J. Nathan, R.M. Kelso

School of Mechanical Engineering
The University of Adelaide, SA 5005, AUSTRALIA

Abstract

A plate with a large aspect ratio nozzle was mechanically oscillated in a near sinusoidal fashion with three ratios of oscillation stroke to nozzle diameter, namely 10, 5 and 2.5. A set of 210 different flow conditions was investigated in the laminar Reynolds number regime and visualized utilizing both the hydrogen bubble and dye trace technique. Three flow regimes were identified with the transition between them being dependent on a Strouhal number based on oscillation stroke, which is equivalent to a relative velocity ration of the plate to the jet, |V|/U. The first regime identified occurs in the highest velocity ratio region and has been termed the Wall Vortex regime. Here a vortex detaches from the jet at the end of each stroke and stays attached to the plate. A second flow regime, termed the Mushroom Vortex regime exists at lower velocity ratios. Here a counter-rotating vortex pair forms within the jet at the end of each stroke. The third regime is called the Weaving Jet regime. Here the jet is ejected approximately normal to the plate but exhibits large-scale oscillations further downstream. All regimes were recorded and half sequences are presented here.

Introduction

Jets find common usage in chemical and combustion processes, for example, and have therefore been widely studied. The orderly structures and flow instabilities within them have received special attention because they dominate the rate of spread and decay, etc. However, most research on the subject has been undertaken on round jets. Throughout the past decades it has been shown that it is possible to excite jets by acoustical [2], fluidic [10] and mechanical means [8]. Of these, the fluidic excitation has the greatest potential for application in harsh industrial environments, typically of furnaces and kilns, although each may have its niche. Significantly, relatively little effort has been spent on the investigation of stimulated planar jets and likewise, relatively few practicable applications have been conceived. One such device, which uses fluidic excitation is the planar flip-flop nozzle of Mi *et al*. [7]. This has been shown to yield significantly higher initial entrainment of the ambient fluid and initial spreading as well as an increase in large-scale mixing. While fluidically excited nozzles such as this are mechanically robust and can be employed in high temperature processes, they are not well suited to rigorous investigations at fundamental level. For example the oscillation frequency depends directly on the jet velocity and geometry, so preventing the possibility of their individual variation. In addition, the velocity profiles at the nozzle exit are neither uniform nor well defined, even if the inlet flow is.

In contrast, mechanically oscillated planar jets can be well defined and have been investigated since the 1970s. Simmons *et al.* [9] and Collins *et al.* [1] developed an apparatus consisting of a plenum chamber with a smooth contracting nozzle (length to height ratio, i.e. nozzle aspect ratio of 60) and a large oscillating vane positioned in the potential core.

This imposed an angular oscillation on the jet, resulting in higher initial jet spread and bulk fluid entrainment. Although the apparatus allowed for independent variation of the oscillation frequency and jet velocity, an angular velocity was introduced by the flapping of the vane increasing the complexity of the investigation. To reduce this complexity, a modified apparatus was employed by Galea [3] and Galea & Simmons [4]. Here one of the nozzle plates was oscillated instead of a flapping vane , so modulating the nozzle width. Again an increase in jet spreading angle and bulk fluid entrainment was shown. The stroke of oscillation to nozzle diameter ratio was chosen to be ≤ 0.1. These investigations as well as all other currently know investigations were undertaken at a St ~ 0.3 trying to achieve the maximum amplification as described by [2].

To the authors' current knowledge, no investigations been performed on a large aspect ratio oscillating nozzle with a stroke to nozzle diameter ratio greater than unity. To address this issue the present study performs a flow visualization study using a mechanical device to identify the flow regimes for a much wider range of oscillations then has been previously assessed.

Experimental Set-up

Experiments were conducted in a water tunnel facility using dye traces or a hydrogen bubble wire as flow visualisation techniques. The oscillating plate (figure 1) consists of a sliding plate with a smooth radially contracting nozzle of aspect ratio, w/h = 16.5. It is driven by a crank-conrod mechanism with a near sinusoidal motion that provides a maximum motion deviation from pure simple harmonic motion (SHM) of 10%. The stroke length (S) to nozzle height (h) ratios (R) investigated were 10, 5 and 2.5. By using the nozzle height to calculate the Reynolds number, the flows investigated were in the range Re = 253 - 1831. The frequencies of oscillation ranged from 0.25 Hz - 1.25 Hz. The flow visualization experiments were recorded with a 0.47-mega-pixel digital video camera resolving a pixel size of 0.7mm × 0.7 mm in the case of the hydrogen bubble wire set-up and phase locked still images using a 6-mega-pixel digital SLR camera with a 50 mm standard lens resolving a pixel size of 0.28mm × 0.28 mm. A set of 210 experimental conditions was investigated for different combinations of oscillation frequency, stroke to diameter ratios and Re using the hydrogen bubble wire method (Table 1). All recorded cases were examined to identify characteristic flow features. A limited set of conditions was repeated using dye visualization to confirm observations made in the preliminary experiments and to provide higher quality images.

Dye flow visualization experiments used a rake of small probes positioned stationary upstream from the oscillating plate along the vertical nozzle centreline to achieve evenly distributed dye flow through the nozzle. For both, the hydrogen bubble wire and dye, no buoyancy effect of the marker particles were noted.

The oscillation of the plate translates the source of the jet with a perpendicular velocity, in a manner that closely approximates SHM and hence can be calculated as

$$V_i = \frac{S}{2} \times (2 \times \pi \times f) \times \cos(t \times 2 \times \pi \times f) \qquad (1)$$

where

V_i = Instantaneous plate velocity (m.s^{-1});
S = Oscillation stroke (m);
f = Oscillation frequency (Hz);
t = Time (s);

whereby the oscillation stroke is equal to twice the amplitude. Although V_i varies with time, for the purpose of a comparative study it is possible to characterize it based on the maximum value, |V|, at the centreline position, eliminating the cosine term from *(1)*.
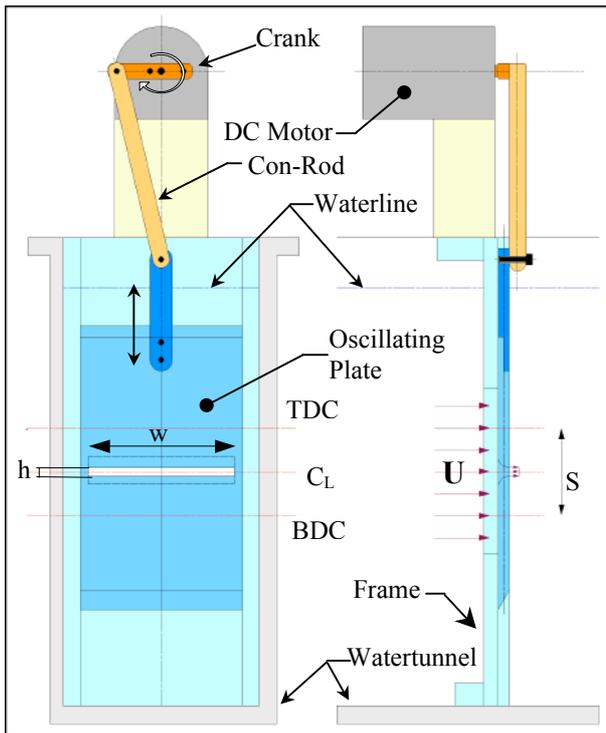
Figure 1. Mechanically Oscillating Planar Jet mechanism. S = oscillation stroke; C_L = oscillation centreline; TDC = top dead centre; TDC = bottom dead centre; h = nozzle width; w = nozzle length; U = jet mean velocity.

Variable	Unit	Values
Oscillation Frequency (f)	Hz	0.25 – 1.25 (Increments of 0.25 Hz)
Stroke/ Diameter Ratio (R)		10, 5, 2.5
Reynolds Number (Re_h)		253 – 1831 (Increments of 126)

Table 1. Investigation grid for hydrogen bubble wire flow visualisation experiments.

Flow Regimes

From recorded footage one of three dominant flow regimes was found to exist in all of the amplitude-nozzle ratios investigated. These regimes have been termed, as follows

- the Wall Vortex regime
- the Mushroom Vortex regime
- the Weaving Jet regime

The ratio of the characteristic |V|/U, is equivalent to a Strouhal number based on the oscillation amplitude. As shown

$$St_S = \frac{|V|}{U} = \frac{S \times f}{U} \qquad (2)$$

appears to be one of the most important scaling parameters. The characteristic features and conditions under which they occur, are assessed in turn.

Wall Vortex Regime

A time sequence spanning a half- cycle of oscillation in the wall vortex regime is shown in figure 6. Note that the images of the flow have been rotated by 90˚ (to appear vertical) to assist in formatting the images in the available space. During the phase in the cycle, when the nozzle passes the oscillation centre line and the nozzle starts to decelerate, a small vortex forms behind the nozzle jet. When the nozzle reaches TDC or BDC, the vortex separates from the jet and remains approximately stationary at the point of detachment. TDC and BDC are the phase in the oscillation (approximately SHM), where the maximum deceleration followed by the maximum acceleration occurs. The vortex dissipates during the subsequent cycle and cannot be identified visually as a coherent feature by the phase in the

oscillation cycle when the nozzle reaches the opposite turning point. During the phase where the vortex can be identified as a coherent feature by visual inspection, it seems to grow steadily by entraining ambient fluid throughout the phase the vortex appears to be attached to the plate surface. Shortly before transition into the next regime a small counter- rotating vortex appears between the main vortex and the plate (figure 2), which is then "squashed" by the larger vortex. The Wall Vortex regime is situated in the highest range of $|V|/U$ of the currently investigated cases.
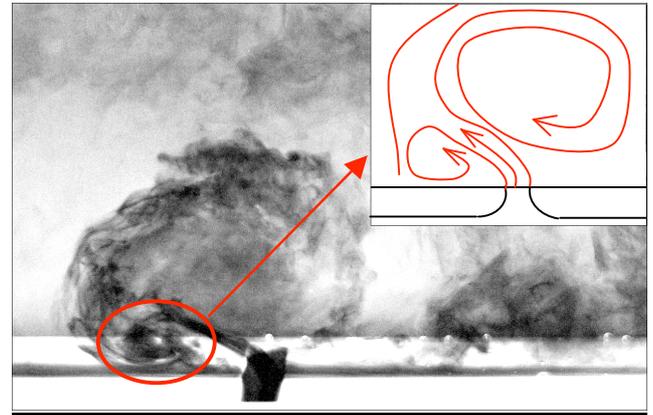

Figure 2. Wall vortex regime shortly before detachment of vortex structure and transition to the mushroom regime.

Mushroom Vortex Regime

The mushroom vortex regime exists at a |V|/U range below the range of the wall vortex regime for each R. In this regime the jet momentum high enough to prevent the vortex formed at TDC and BDC from being attached to the oscillating plate and to form a counter- rotating vortex pair (figure 7). The motion of the plate causes the apparent angle between the jet and the plate to be large. However it should be noted that velocity measurements are required to obtain actual trajectories. The mushroom shape of the formed vortices bear some resemblance with vortex rings formed described by such likes as [5] (figure 3).
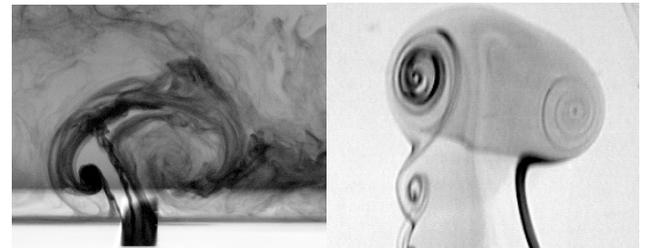

Figure 3. Mushroom vortex from mechanically oscillated planar jet (left) and vortex rings from jet as described by [5] (right) (Photo: E. Hassan [6]).

Figure 4. Jet in the weaving jet regime with inclusion of the flow field further downstream. Initially nearly straight jet shows high degree of oscillation in the far field.

Weaving Jet Regime

The weaving jet regime occurs at a |V|/U range below the mushroom vortex range (figure 8). This regime is related to the mushroom vortex regime and in addition to the jet being more perpendicular to the oscillating plate during its initial ejection phases, the main difference is that no visible counter-rotating vortex pairs exist here. The initial near field of the jet is visually very similar to a steady flow jet, with two important differences. Firstly, the shear layer vortices are strongly magnified compared to a steady jet and secondly, they are larger on the trailing edge of the oscillating jet. Inspections of the flow field downstream from the initially straight jet (figure 4) shows that it subsequently develops a large-scale oscillation.
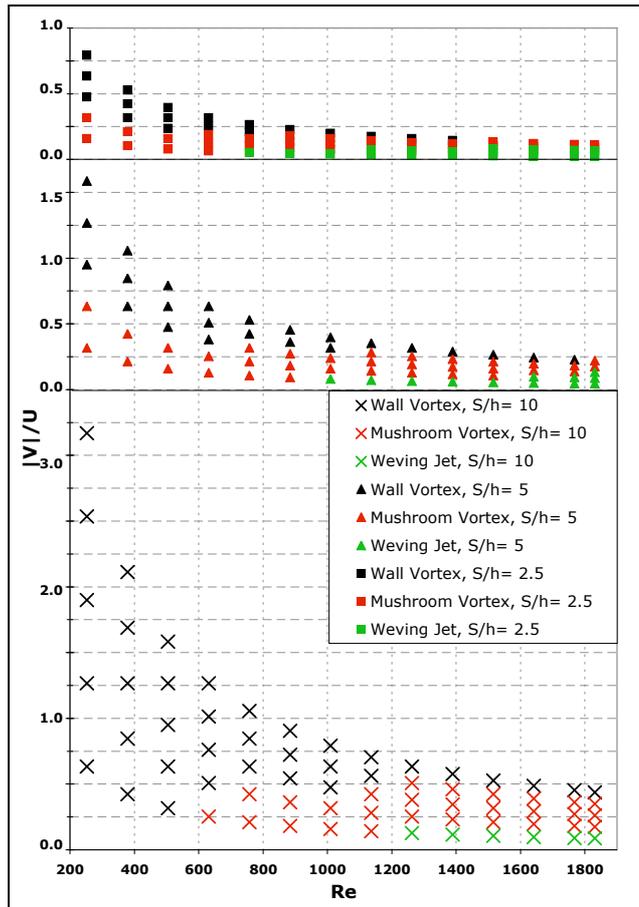

Figure 5. Flow regimes as identified for different s/h.

Regime Boundaries

A systematic study was performed to identify which regime occurs in each of a wide combination of Re, *R* and |V|/U. These were all performed with a fixed nozzle, so that varying the stroke causes a variation in *R*. The technique chosen for this investigation was the hydrogen bubble. The results can be seen in figure 5.

It can be seen that as expected the flow regimes follow the same sequence from Wall Vortex over Mushroom Vortex to Weaving Jet for all *R*. For each value of *R* regime boundaries seem to approach a constant value with increasing Re as the influence of viscous forces is reducing and it is expected that this trend continues in the transition and turbulent regime. However it can also be seen that for constant Re the regime boundaries are changing at different values of |V|/U for different *R*.

As all tests were carried out over a grid of discrete $|V|/U$ values, which were determined prior to any knowledge of the flow to be encountered and solely governed by the achievable values, entrenched in the mechanical properties of the experimental apparatus are hence making it impossible to exactly determine the regime boundaries from the existing data.

As the three regimes do not suddenly change from one into the other, but rather gradually approach a different regime under varying flow conditions and hence the determination of the mode in each case was somewhat subjective. At the current moment it is unclear if any further flow regimes exist and what their characteristics are.

Conclusions

From flow visualization of the transverse oscillation of the source of a planar jet, three flow regimes were identified and characterized. These flow regimes have not been documented previously and exhibits considerable differences to the flows observed by related investigations [3, 4, 9]. It should be noted that the present investigations were undertaken with a relatively small nozzle aspect ratio with a facility that was only able to produce flows in the laminar Re regime. Further investigations are planned with a new facility that provides better-controlled initial conditions, such as minimizing three-dimensional end-effects from the nozzle, and is also capable of operating within the turbulent Re regime. This work will redefine the regime boundaries and provide further detailed of each the flow regimes identified.

References

[1] Collins, D J, Platzer, M F, Lai, J C S & Simmons, J M, Experimental Investigations of Oscillating Subsonic Jets, *Conference Proceedings of Numerical and Physical Aspects of Aerodynamic Flows*, 1982, pp 575 – 587.

[2] Crow, S C & Champagne F H, Orderly Structures in Jet Turbulence, *Journal of Fluid Mechanics*, No 3, Vol 48, Aug 1971, pp 547 – 591.

[3] Galea, S C, *Excitation of a Plane Turbulent Jet by Nozzle Area Variation*, Master Thesis, University of Queensland, Australia, May 1983.

[4] Galea, S C & Simmons, J M, Excitation of a Plane Jet by Periodic Perturbation of the Nozzle Area, *Eighth Australasian Fluid Mechanics Conference*, 1983, 13C.5 - 13C.8.

[5] Gharib, M, Rambod, E & Shariff, K, *A universal time scale for vortex ring formation*, Journal of Fluid Mechanics, Vol 350, Apr. 1998, pp 121 –140.

[6] Hassan, E & Riese, M, Personal unpublished communication, July 2004.

[7] Mi, J, Nathan, G J, & Luxton, R E, Dynamic Oscillation of a Quasi-Planar Jet, *12th Australasian Fluid Mechanics Conference*, 1995, pp 119 – 122.

[8] Schneider, G M, *Structures and turbulence characteristics in a precessing jet flow*, PhD Thesis, University of Adelaide, Australia, 1996.

[9] Simmons, J M, Lai, J C S & Platzer, M F, Jet Excitation by an Oscillating Vane, *AIAA Journal*, No 6, Vol 19, June 1981, pp 673 – 676.

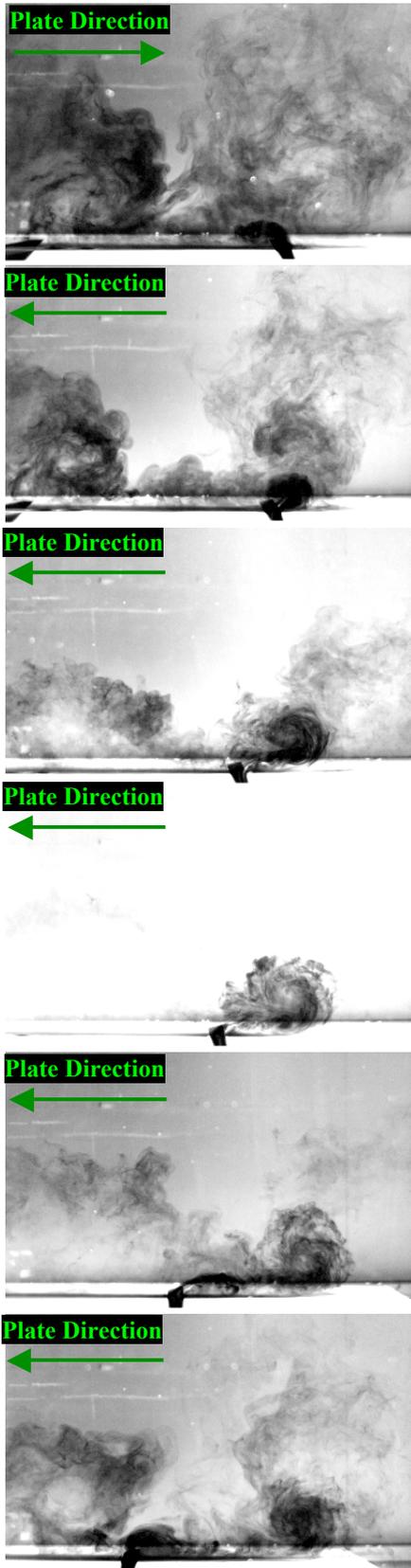[10] Viets, H, Flip-Flop Jet Nozzle, *AIAA Journal*, No 10, Vol 13, Oct 1975, pp 1375-1379.

Figure 6. Pseudo sequence of a jet in the wall vortex flow regime (top to bottom). Vortex forms at TDC and BDC and stays attached to plate. Flow symmetrical across oscillation centreline.
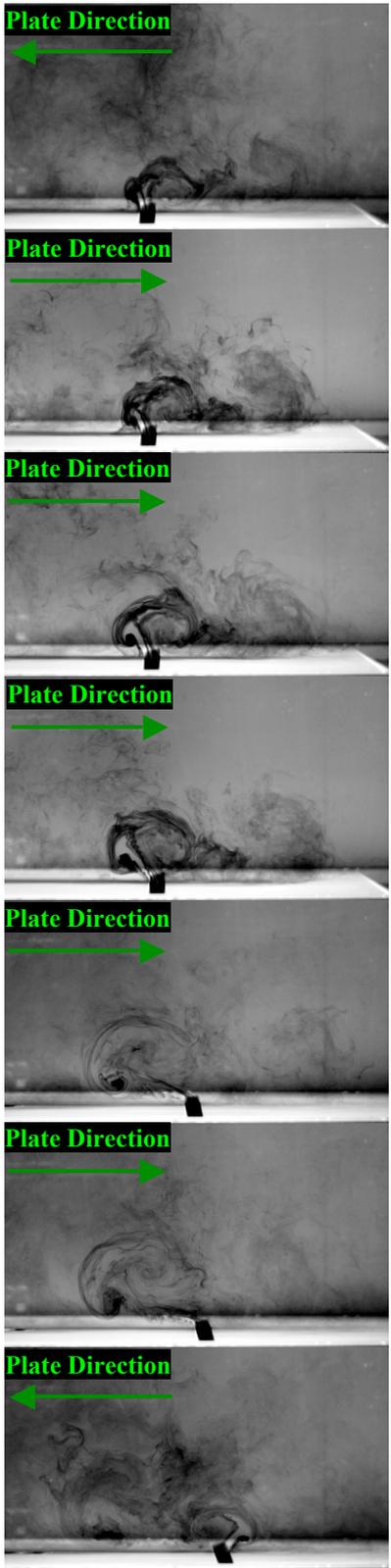

Figure 7. Pseudo sequence of a jet during the mushroom vortex flow regime (top to bottom). Jet forms counter-rotating vortex pair at TDC and BDC, which is detached from the oscillating plate. Flow symmetrical across oscillation centreline.
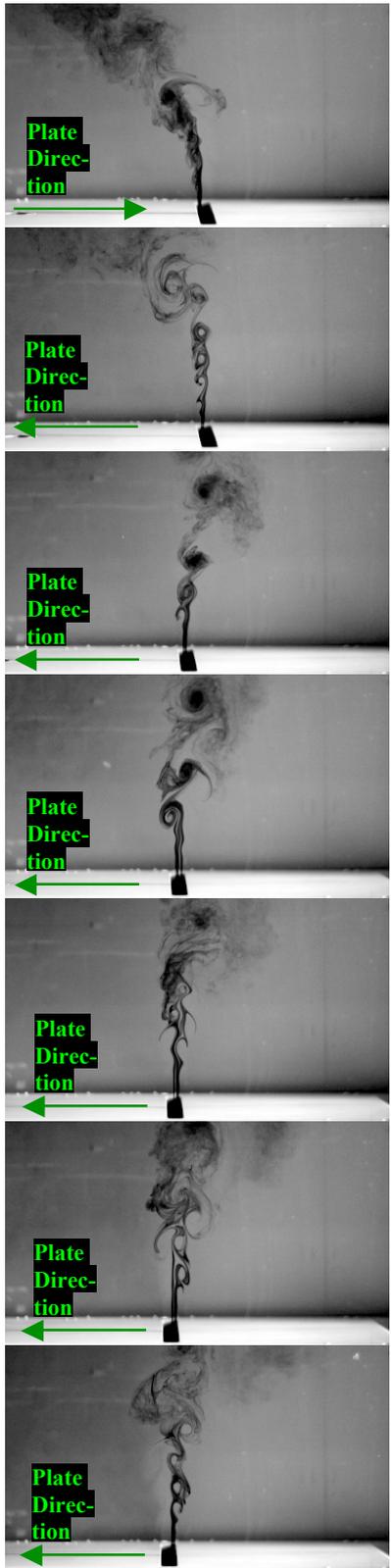

Figure 8. Pseudo sequence of a jet during the weaving jet flow regime (top to bottom). Jet does not form visible counter-rotating vortex pairs at TDC and BDC, shear layer vortex structures appear magnified on trailing edge of jet compared to steady jet flow. Flow symmetrical across oscillation centreline.